Photoconductive Properties of $GaAs_{1-x}N_x$ Double Heterostructures as a Function of Excitation Wavelength

R. K. Ahrenkiel*, A. Mascarenhas*, S. W. Johnston*, Y. Zhang*, D. J. Friedman*, and S. M. Vernon**
*National Renewable Energy Laboratory
**Spire Corporation

ABSTRACT

The ternary semiconductor $GaAs_{1-x}N_x$ with $0 < x < 0.3$ can be grown epitaxially on GaAs and has a very large bowing coefficient. The alloy bandgap can be reduced to about 1.0 eV with about a 3% nitrogen addition. In this work, we measured the internal spectral response and recombination lifetime of a number of alloys using the ultra-high frequency photoconductive decay (UHFPCD) method. The data shows that the photoconductive excitation spectra of the $GaAs_{0.97}N_{0.03}$ alloy shows a gradual increase in response through the absorption edge near E_g. This contrasts with most direct bandgap semiconductors that show a steep onset of photoresponse at E_g. The recombination lifetimes frequently are much longer than expected from radiative recombination and often exceeded 1.0 μs. The data was analyzed in terms of a band model that includes large potential fluctuations in the conduction band due to the random distribution of nitrogen atoms in the alloy.

INTRODUCTION

The ternary alloy $GaAs_{1-x}N_x$ is of current interest because of the rapid decrease of bandgap with very small nitrogen concentrations. For nitrogen concentrations of $0 < x < 0.03$, the bandgap E_g in eV decreases approximately as[1]:

$$\Delta E_g(x) = b(x)\, x(x-1)\ (\text{eV}) \qquad (1)$$

where x is the fractional nitrogen concentration N_x and the bowing coefficient b(x) is composition dependent and varies between 10 and 20 eV. For a 3.0 % nitrogen alloy, the bandgap of $GaAs_{1-x}N_x$ decreases to about 1.0 eV. These alloys have technological interest as a 1.0-eV direct-bandgap semiconductor.

Key parameters for potential applications of these alloys are the electronic transport properties, including the carrier mobilities and electron-hole recombination rates (recombination lifetime).

In this work, we have measured the in-plane photoconductive lifetimes using the contactless ultra-high-frequency photoconductive decay (UHFPCD) technique. Descriptions of this technique have been described in the literature[2, 3, 4]. Using a variable-wavelength excitation source, we use the UHFPCD method to measure the internal spectral response. The light source is a Coherent Radiation optical parametric oscillator (OPO, model XPO) pumped by a tripled Coherent Infinity YAG laser. In the idler mode, this light source provides wavelengths from 711 nm to 2200 nm. For these studies, we measured the transient photoconductive decay over a wide range of wavelengths.

The theoretical understanding of the physics of bandgap reduction and the large bowing coefficient is of considerable interest. Using electroreflectance, Perkins and coworkers [5] observed the bandgap transition (E_0) and a transition from the spin-orbit split-off valence band ($E_0 + \Delta$). They also observed a higher-energy transition, labeled E_+, for nitrogen concentrations of $x > 0.008$. The

Mat. Res. Soc. Symp. Proc. Vol. 607 © 2000 Materials Research Society

Downloaded from https://www.cambridge.org/core. Univ. of North Carolina at Charlotte, on 03 Aug 2018 at 15:43:54, subject to the Cambridge Core terms of use, available at https://www.cambridge.org/core/terms. https://doi.org/10.1557/PROC-607-265

valence spin-orbit splitting Δ is nearly independent of N concentration, indicating that the nitrogen interacts primarily with the conduction band. They suggest that E_+ is a nitrogen impurity band as E_+-E_0 increases with increasing N concentration. The E_+ level could originate from a resonant level in the conduction band or from a disorder-activated indirect transition. Shan and coworkers [6] have proposed that the anti-crossing interaction between a localized nitrogen state and the conduction-band states produces the bandgap reduction in $Ga_{1-x}In_xN_yAs_{1-y}$ alloys. Here, small concentrations of In are added for lattice matching to GaAs. For example, the quaternary compound $Ga_{0.95}In_{0.05}N_{0.02}As_{0.98}$ is lattice matched to GaAs. This compound was shown by Geisz and coworkers[7] to produce quantum efficiencies (QE) of less than 0.14 when used as the absorbing layer in a liquid-junction device. These data indicated short diffusion lengths, with collection only from carriers generated in the high electric field of the depletion region.

Here, we will present the photoconductive decay data to analyze in-plane transport properties of $GaAs_{1-x}N_x$. The samples were all grown as isotype double-heterostructures (DH) with the structures $GaAs/GaAs_{1-x}N_x/GaAs$ or $GaInP/GaAs_{1-x}N_x$ /GaInP on semi-insulating GaAs substrates. The $GaAs_{1-x}N_x$ epitaxial layers are p-type when not intentionally doped. Films were grown by metal-organic chemical vapor deposition (MOCVD) at Spire Corporation and at NREL using dimethylhydrazine as a nitrogen source.

The UHFPCD technique measures the transient photoconductivity (pc) following excitation from a pulsed light source. The pc after pulsed excitation is:

EXPERIMENATAL

$$\Delta\sigma = q(\mu_n + \mu_p)\rho(t) \qquad (2)$$

Here, μ_n and μ_p are the electron and hole mobilities respectively, and $\rho(t)$ is the excess carrier concentration. When the recombination mechanism can be written in terms of a single lifetime τ, then:

$$\Delta\sigma = q(\mu_n + \mu_p)\rho_0 \exp(-t/\tau) \qquad (3)$$

Here, ρ_0 is the initial light-induced excess electron (hole) density. The minimum lifetime resolution, with the current UHFPCD apparatus, is about 40 ns, which we designate as the system response. The free-carrier decay time is frequently, if not almost always, nonexponential and depends on injection level. Such effects will be prominent in these data.

The spectral response at a given wavelength is defined by the time integral of the transient decay:

$$Q = \int_0^{t_{max}} \Delta\sigma(t)\, dt. \qquad (4)$$

In these measurements, the transient signal is averaged and stored by a digital processing oscilloscope.

An advantage of this technique is that we can measure the photoconductive properties of an electrically isolated region of the device. We detect the photo-induced currents that are confined to an electrically isolated region such as at the active region of an isotype double-heterostructure. Thus, the quantum efficiencies measured by this technique will differ from those that require current flow to an external circuit. We have designated the transient data, when integrated by Eq. 4, as the internal spectral response.

Downloaded from https://www.cambridge.org/core. Univ. of North Carolina at Charlotte, on 03 Aug 2018 at 15:43:54, subject to the Cambridge Core terms of use, available at https://www.cambridge.org/core/terms. https://doi.org/10.1557/PROC-607-265

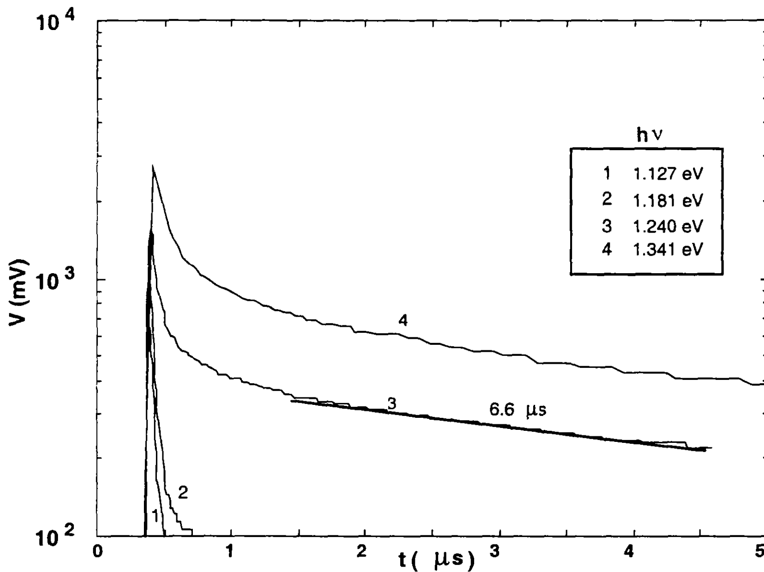

Fig. 1. The time-resolved photoconductivity of sample A (x = 0.01) with the excitation source tuned to selected wavelengths. The photon energies, corresponding to these wavelengths, are indicated in the figure.

The data of Fig. 1 were measured on a sample (A) grown at NREL using MOCVD. The structure is a GaAs/$GaAs_{0.99}N_{0.01}$/GaAs DH on a chromium-doped GaAs substrate. The GaAsN layer thickness is 0.4 μm and is p-type with a hole density of about 1 x 10^{17} cm^{-3}. The onset of photoconductivity occurs for hν > 0.9 eV but an abrupt change in behavior is observed at about 1.2 eV. The photoconductive lifetimes for hν < 1.2 eV are very short and nearly equal to system response, as shown by curves 1 and 2. For hν > 1.2 eV, the response increases rapidly, with much larger decay times. The long-term decay for curves 3 and 4 shows a lifetime of greater than 6 μs. The increased decay times occur for hν > E_g, the bandgap of the alloy. The radiative decay time for epitaxial GaAs, doped to 1 x 10^{17} cm^{-3}, is about 50 ns. The larger lifetime found for this series of samples will be discussed later in this section.

Sample B is a DH grown at the Spire Corporation by MOCVD and contains about 3.3 % nitrogen. The $GaAs_{0.97}N_{0.03}$ layer thickness is 0.2 μm, and the conductivity of the sample is p-type (3 x 10^{17} cm^{-3}) as measured by the capactiance-voltage method. Fig. 2 shows the photoconductive response of sample B at six incident photon energies (0.827 eV) to 1000 nm (1.24 eV). These are labeled curves 1 through 6 in the figure. Curves 1, 2, and 3 represent photon energies less than the bandgap of 1.00 eV. The transient response shows an initial fast decay, followed by a second slower decay. Curve 4 is the data for hν = 1.033 eV, and the fast

Downloaded from https://www.cambridge.org/core. Univ. of North Carolina at Charlotte, on 03 Aug 2018 at 15:43:54, subject to the Cambridge Core terms of use, available at https://www.cambridge.org/core/terms. https://doi.org/10.1557/PROC-607-265

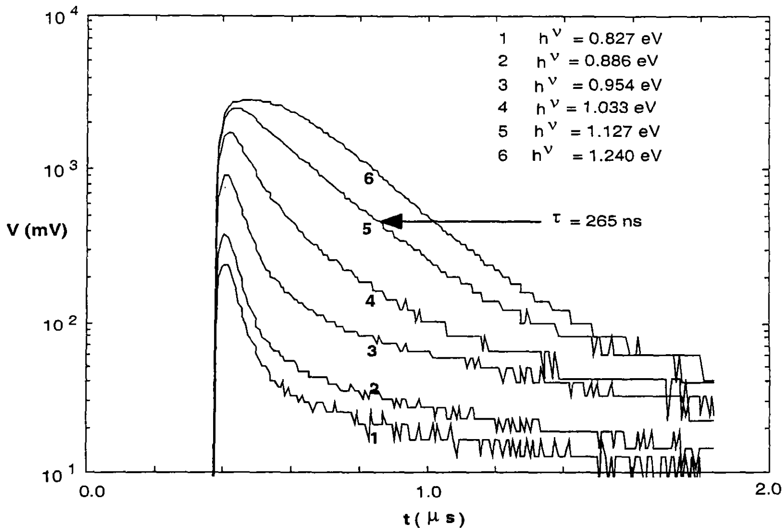

Fig. 2. The time-resolved photoconductivity of sample A (x = 0.033) with the excitation source tuned to selected photon energies as shown.

component has nearly disappeared. Curves 5 and 6 represent the data for hν = 1.127 eV and hν = 1.240 eV, respectively. In this excitation range, the decay time becomes about 264 ns and is nearly exponential in character. Of course, we do not know the radiative recombination coefficient of this alloy that represents transitions from the perturbed conduction band to the valence band. For GaAs at the doping level, the radiative lifetime is about 17 ns[8].

Figure 3 shows the internal spectral response of both of these samples that is obtained by integrating the transient data with Eq. 4 over the entire data set of excitation wavelengths (photon energies). The data set was normalized to the relative density of incident photons/cm^2 at each wavelength. The incident photon intensity was highly attenuated by means of filters to keep the response in the low carrier-injection range. Curve A represents sample A and shows a weak onset of photoconductive response at 0.9 eV. A fairly steep increase in photoconductivity is observed at about 1.2 eV, corresponding to the expected bandgap of this composition. A weak drop in response is observed at 1.27 eV, followed by a more gradual increase in response up to the GaAs bandgap. Curve B represents the photoconductive response of sample B. Here, the weak onset of photoconductivity is seen at about 0.75 eV. At 0.9 eV, the slope of Q vs. hν increases suddenly and continues through the bandgap range up to about 1.25 eV. The slope in this range is much lower than that of curve A in the range of the expected bandgap. At about 1.36 eV, there is a steep drop in response of sample B, followed by a sharp rise in response up to the GaAs bandgap. The DH structures with a GaInP window layer allowed measurements up to about 1.75 eV, with no further significant change of photoconductive behavior.

Downloaded from https://www.cambridge.org/core. Univ. of North Carolina at Charlotte, on 03 Aug 2018 at 15:43:54, subject to the Cambridge Core terms of use, available at https://www.cambridge.org/core/terms. https://doi.org/10.1557/PROC-607-265

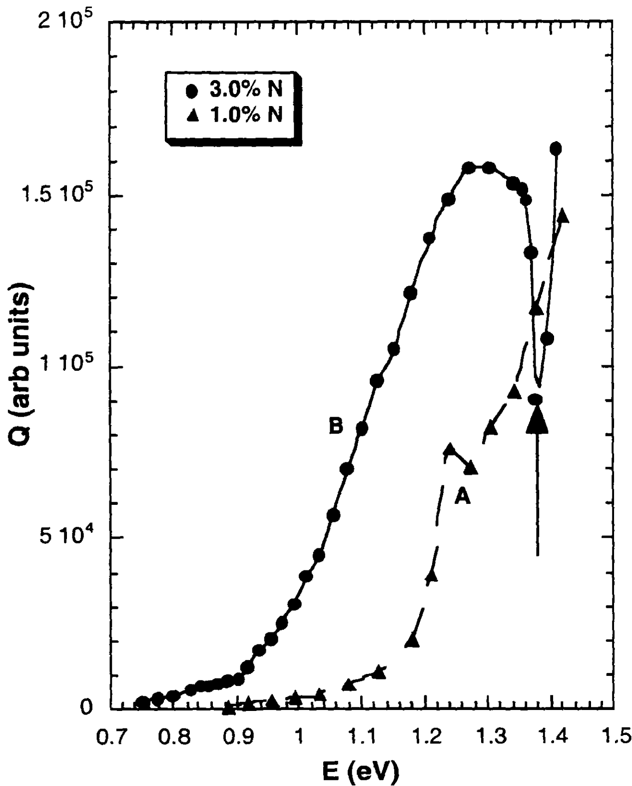

Fig. 3. The internal spectral response of two GaAs/$GaAs_{1-x}N_x$ /GaAs structure grown by MOCVD. Curve A: p-type (~1 $x10^{17}$ cm^{-3}) and x ~ 0.01. Curve B: p-type (~3 $x10^{17}$ cm^{-3}) and x = 0.03.

Discussion of Results

The nature of electron transport in the ternary $GaAs_{1-x}N_x$ is complex owing to the unknown, but apparently complex structure of the conduction band. There were no significance differences seen for DHs with GaAs and GaInP window layers. The relatively large photoconductive recombination lifetimes are surprising based on the observations of Geisz and coworkers[7] of very weak external spectral response and minority-carrier diffusion length. Applying the radiative (B coefficient) of GaAs, the predicted radiative lifetime both samples is 50 ns or

Downloaded from https://www.cambridge.org/core. Univ. of North Carolina at Charlotte, on 03 Aug 2018 at 15:43:54, subject to the Cambridge Core terms of use, available at https://www.cambridge.org/core/terms. https://doi.org/10.1557/PROC-607-265

less, much shorter than seen here. These data can be reconciled with that of Geiss, et al if one assumes that the electron motion is highly localized in nitrogen-perturbed conduction bands, whereas the hole motion is uninhibited by a relatively unperturbed valence band. The electron moves by "hopping" electron transport between spatial potential wells containing nitrogen clusters.

The large recombination lifetime can be attributed to several possible physical mechanisms. First, recombination may be inhibited by the charge separation effect produced by the localized potential fluctuations that comprise the conduction band. Second, the matrix elements that connect conduction and valence band states may be weakened by the interaction with the nitrogen states.

Figure 4 shows a possible model that is similar to that proposed by Anderson[9] for impurity bands in doped semiconductors. Here, however, the potential wells are much deeper because of the large interation between the GaAs conduction band states and the accidentally degenerate nitrogen levels. Variations in the localized alloy composition can be described using the distribution function of Holtsmark[10]. The resulting variation in alloy composition causes potential fluctuations in the perturbed conduction band. One effect of the potential fluctuations may be the charge separation of electrons and holes. Buyanova and coworkers[11] showed by photoluminescence studies that the free carriers appeared to be confined and that a charge-separation mechanism existed. Preliminary temperature-dependent photoconducitve studies of $GaAs_{1-x}N_x$ have shown large increases in the recombination lifetime at temperatures below about 150 K. Similar effects have been observed in photoconductive decay containing order/disorder domains in InGaAs[12,13,14].

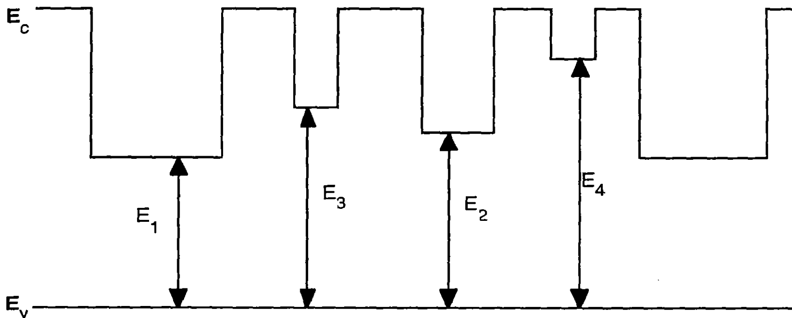

Fig. 4. A proposed band structure of the $GaAs_{1-x}N_x$ alloy that includes a random distribution of localized nitrogen concentrations. The bandgap varies with cluster size.

The data of Fig. 3, Curve B, show that the rise of photoconductivity in $GaAs_{0.97}N_{0.03}$ is much less abrupt than in $GaAs_{0.99}N_{0.01}$. This behavior is consistent with the model of Fig. 4. Here, we attribute this photoconductive behavior to the inhomogeneity of the localized nitrogen concentration. The lowest energy response comes from regions of the highest nitrogen content. According to the Holtsmark distribution model, the number of regions of a given impurity content will decrease inversely with the impurity density of those regions. Thus, Fig. 3, Curve B, shows the photoconductive response increasing with increasing photon energy, reflecting the relative increase in number density of lower impurity density regions.

Downloaded from https://www.cambridge.org/core. Univ. of North Carolina at Charlotte, on 03 Aug 2018 at 15:43:54, subject to the Cambridge Core terms of use, available at https://www.cambridge.org/core/terms. https://doi.org/10.1557/PROC-607-265

CONCLUSIONS

In summary, the internal spectral response and transport in $GaAs_{1-x}N_x$ is very complex. The data suggest a random distribution of nitrogen atoms in the alloy, which produces large conduction-band fluctuations. These fluctuations inhibit the motion of electrons, but have little effect on the valence-band holes. The latter produce strong photoconductive effects in the alloy system. The electron-hole recombination rate is reduced by the perturbed conduction band through several possible mechanisms.

REFERENCES

1. A.B. Chen and A. Sher, *Semiconductor Alloys Physics and Materials Engineering*, Plenum Press, New York, 1995.

2. R. K. Ahrenkiel, R. Ellingson, S. Johnston, and M. Wanlass, Appl. Phys.Lett. **72**, p. 3470 (1998).

3. R. K. Ahrenkiel and S. Johnston, Solar Energy Materials and Solar Cells **55**, p. 59 (1998).

4. R. K. Ahrenkiel, U. S. Patent 5,929,652, (July 27, 1999).

5. J. D. Perkins, A. Mascarenhas, Y. Zhang, J. F. Geisz, D. J. Friedman, J. M.Olson, and S. R. Kurtz, Phys. Rev. Lett. **82**, p. 3312 (1999).

6. W. Shan, W. Walukiewicz, J. W. Ager III, E. E. Haller, J. F. Geisz, D. J.Friedman, J. M. Olson, and S. R. Kurtz, Phys. Rev. Lett. **82**, p. 1221 (1999).

7. J. F. Geisz, D. J. Friedman, J. M. Olson, S. R. Kurtz, and B. M. Keyes, J.Crystal Growth **195**, p. 401 (1998).

8. R. K. Ahrenkiel in *Minority Carriers in III-V Semiconductors: Physics and Applications*, SEMICONDUCTORS AND SEMIMETALS, V. 39, Academic Press (1993), R.K. Ahrenkiel and M. S. Lundstrom, editors, p. 131.

9. P. W. Anderson, Phys. Rev. **109**, p. 1492 (1958).

10. J. Holtsmark, A., Physik **59**, p. 577 (1919).

Downloaded from https://www.cambridge.org/core. Univ. of North Carolina at Charlotte, on 03 Aug 2018 at 15:43:54, subject to the Cambridge Core terms of use, available at https://www.cambridge.org/core/terms. https://doi.org/10.1557/PROC-607-265